Signal enhancement in optical projection tomography via virtual high dynamic range imaging of single exposure

Yujie Yang[a], Di Dong[a], Liangliang Shi[a], Jun Wang[b], Xin Yang[a], Jie Tian[*a]

[a]Key Laboratory of Molecular Imaging of Chinese Academy of Sciences, Institute of Automation, Chinese Academy of Sciences, Beijing 100190, China; [b]Harbin University of Science and Technology University, Automation Engineering School, Harbin 150080, China

ABSTRACT

Optical projection tomography (OPT) is a mesoscopic scale optical imaging technique for specimens between 1mm and 10mm. OPT has been proven to be immensely useful in a wide variety of biological applications, such as developmental biology and pathology, but its shortcomings in imaging specimens containing widely differing contrast elements are obvious. The longer exposure for high intensity tissues may lead to over saturation of other areas, whereas a relatively short exposure may cause similarity with surrounding background. In this paper, we propose an approach to make a trade-off between capturing weak signals and revealing more details for OPT imaging. This approach consists of three steps. Firstly, the specimens are merely scanned in 360 degrees above a normal exposure but non-overexposure to acquire the projection data. This reduces the photo bleaching and pre-registration computation compared with multiple different exposures in conventional high dynamic range (HDR) imaging method. Secondly, three virtual channels are produced for each projection image based on the histogram distribution to simulate the low, normal and high exposure images used in the traditional HDR technology in photography. Finally, each virtual channel is normalized to the full gray scale range and three channels are recombined into one image using weighting coefficients optimized by a standard eigen-decomposition method. After applying our approach on the projection data, filtered back projection (FBP) algorithm is carried out for 3-dimentional reconstruction. The neonatal wild-type mouse paw has been scanned to verify this approach. Results demonstrated the effectiveness of the proposed approach.

Keywords: optical projection tomography, high dynamic range, single exposure, signal enhancement

1. INTRODUCTION

Optical projection tomography (OPT) [1] is the optical equivalent of X-Ray Computed Tomography, known as optical CT. In the past decade, OPT was widely applied to gene expression [2], fluorescent immunohistochemistry and phenotype [3] in various tissues and organisms. OPT has been proven to be a powerful tool for imaging specimens between 1 mm and 10 mm with high resolution and sensitivity [4]. However, some specimens containing a wide range contrast elements may result in poor imaging quality for OPT imaging, especially for emission OPT which collects fluorescence emission views likes Fluorescence Molecular Tomography. And in order to acquire the projection data, the longer exposure for high intensity tissues may lead to over saturation of other areas, whereas a relatively short exposure may cause similarity with surrounding background.

To make up for the shortcomings, some signal enhancement methods are introduced in the OPT system. And high dynamic range (HDR) has been described in [5-6] to image specimens containing widely differing contrast elements, which are both required to scan irradiation specimen several times at different exposures. This would increase the computation complexity of image registration when

[*] Jie Tian; Telephone: 8610-82618465; Fax: 8610-62527995; Email: tian@ieee.org, jie.tian@ia.ac.cn; Website: http://www.mitk.net, http://www.3dmed.net

Medical Imaging 2015: Biomedical Applications in Molecular, Structural, and Functional Imaging, edited by Barjor Gimi, Robert C. Molthen, Proc. of SPIE Vol. 9417, 941724

projection images of the same angle at different exposures are not perfectly aligned and increase the cost of the OPT imaging system to ensure the high precision and stability of the mechanical system. Moreover, the photo bleaching and phototoxicity [7] of specimens are increased for larger irradiation doses, especially for fluorescent protein in emission OPT imaging.

In this paper, we propose a method that acquires one image of each angle above a normal exposure but non-overexposure time. Three virtual channels are produced to make a trade-off between capturing weak signals and revealing more details for OPT imaging. Experiments showed this method can improve the imaging quality of OPT.

2. METHODS

2.1 Challenges in applying the conventional HDR technology on the OPT imaging

The conventional HDR images are usually generated from a set of low dynamic range (LDR) images by computing a weighted average of the aligned input images [8]. For OPT imaging, several images of the same angle of the specimen are acquired at different exposures. One way is to scan several circles at different exposures, which would increase the computation complexity of image registration for projection images of the same angle at different exposures are not perfectly aligned. The other way is to take multiple different exposures at each rotational position, but this needs higher precision and stability of the mechanical system, which would greatly increase the cost of the OPT imaging system. So the first way is usually used to acquire the projection images of different exposures.

After acquiring a set of LDR images of the specimen, HDR images are generated by computing camera response function g as

$$L_i(\boldsymbol{p}) = g(Z_i(\boldsymbol{p})) - In(t_i), \tag{1}$$

where $L_i(\boldsymbol{p})$ denotes irradiance of each input image i at pixel $\boldsymbol{p}$ in the scene, Z_i denotes the i-th input image and t_i is the correspondent exposure time. In equation (1), Z_i and t_i are known. The unknowns are the irradiances L_i, as well as the function g. Then these unknowns can be recovered in a least-square error sense. But all these are based on the assumption that the function g is smooth and monotonic, which may cause some imaging artifacts [9]. And for OPT system, this conventional HDR technology cannot be finished in real time. It must be scanned multiple times to acquire the projection data to make the HDR images. At the same time, the photo bleaching and phototoxicity of specimens are increased for larger irradiation doses, especially for fluorescent protein in emission OPT imaging. In this study, we propose an approach to address these problems.

2.2 Virtual HDR imaging via single exposure

In our method, the projection data is acquired by scanning the specimen in 360 degrees above a normal exposure but non-overexposure as shown in Fig. 1 (c). In this exposure time, high intensity parts are slightly visible and other areas are not over saturation. And before the camera scanning, the projection images of first angle are saved, which show the different exposure degree. The specimen is scanned after the exposure degree similar to Fig. 1 (c) is found.

After the projection data is acquired, three virtual channels [10] are produced for each projection image based on the histogram distribution of interest areas. For each projection image, minimum and maximum are the lowest and highest pixel values of all the projection data respectively. According to the first angle's projection image under the different exposure time, low offset is the 60th percentile of the pixel value, and high offset is the 99th percentile of the pixel value. And the original projection image is divided into three datasets, creating three virtual channels: low I_0, normal I_1, and high I_2 signal channels. I_0 consists of pixel values between minimum and low offset, I_2 consists of pixel values between high offset and maximum and I_1 consists of pixel values between low offset and high offset.

Then each channel is processed to maximize the signal dynamic range by linearly rescaling pixel values between lowest and highest values in each channel to the full gray scale range(for example, 0 to 255 for 8-bit). Finally, three channels are recombined into one virtual HDR image using weighting coefficients as follows:

$$I_{HDR}(\boldsymbol{p}) = \sum_{i=0}^{2} w_i I_i(\boldsymbol{p}). \tag{2}$$

Here, $I_{HDR}(\boldsymbol{p})$ stands for the output after HDR imaging at pixel $\boldsymbol{p}$ in the projection data. w_i denotes the weighting coefficients of input channel I_i. And these weighting coefficients are optimized using a standard eigen-decomposition method. Let A, B, C be the feature vectors corresponding to the input channels, then decomposition is computed and weights are obtained as follows:

$$[V\lambda] = eig(\mathrm{cov}[A, B, C]), \tag{3}$$

and

$$w = (V_i / \sum V_i). \tag{4}$$

Where V_i is corresponding to $\lambda_{\max}$ (dominant eigenvalue) entry in λ of the *i*-th column in the eigenvectors *V*, cov[ ] is a covariance matrix. So the coefficients used for calculating the weight are adjusted as a function of the signal strength of the original image so that the image quality can be enhanced with poor signal strength, while preventing the images with good signal strength from over-saturation. And then a median filter is implemented on the recombined result to remove noise and preserves edges. After applying our approach on the projection data, FBP algorithm [11] is carried out as normal for 3-dimentional reconstruction:

$$f(x,y) = \frac{1}{2}\int_0^{2\pi} d\gamma \int_{-\infty}^{+\infty} |\nu| G(\nu,\gamma) e^{j2\pi\nu t} d\nu \Big|_{t=x\cos\gamma + y\sin\gamma}. \tag{5}$$

Where $f(x,y)$ represents the light attenuation coefficient of the tissue, $G(\nu,\gamma)$ is the Fourier transform of projection measurement of $f(x,y)$ onto the direction γ and $|\nu|$ is a ramp filter applied in the Fourier domain.

The simplified process chat is summarized and shown in Fig. 2.

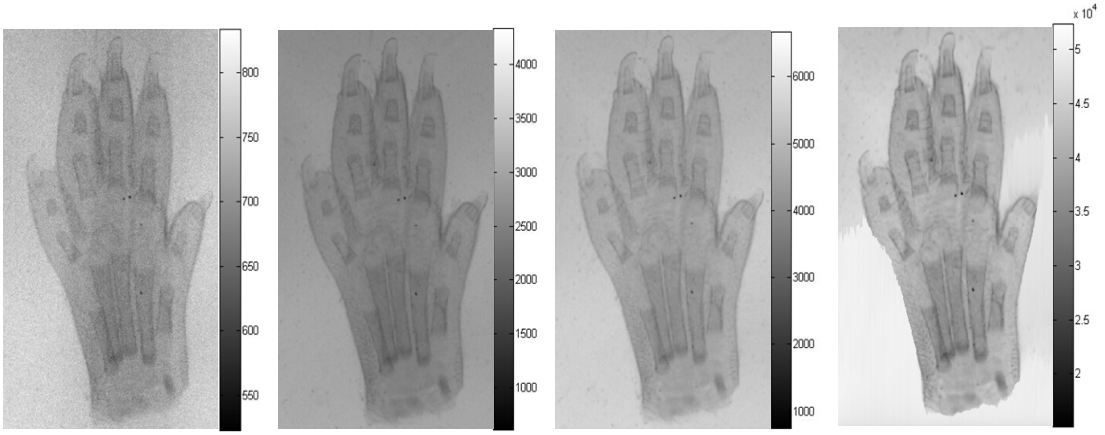

(a) (b) (c) (d)

Figure 1. Projection images of mouse paw in different exposure times: (a) 0.005s, (b) 0.05s, (c) 0.1s, (d) 1s. (a) is in the low exposure with much noise, (b) is usually used as the normal exposure image to make sure that the low-intensity parts of specimen are obtained in a reasonable contrast, (c) is the projection image above a normal exposure but non-overexposure,

(d) is the over-saturation image though the high-intensity parts of mouse paw are clearer.

2.3 Data analysis and display

After reconstruction, the software tool for implementing and analyzing was named 3DMed [12], developed by our group (http://www.3dmed.net/) to integrate the common algorithms of segmentation, registration and visualization.

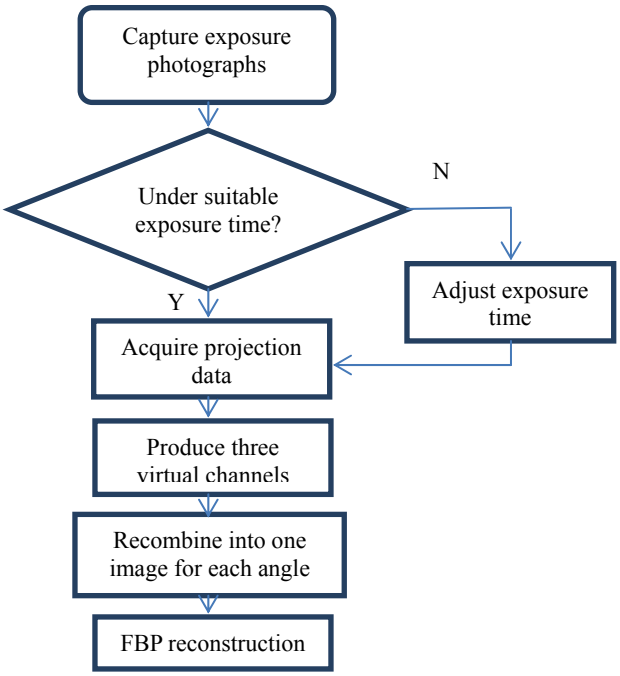

Figure 2. Simplified process chat of the method

3. RESULTS AND DISCUSSION

To test and verify our proposed approach, the data of neonatal wild-type mouse paw was obtained by our OPT prototype system [13]. The mouse paw has been dehydrated and transparency. All animal experiments were conducted in consistence with international, national and institutional laws and guidelines. And the paw is scanned in a single exposure and each projection image is divided into three virtual channels analogous to HDR imaging before reconstruction. Fig. 3 shows the results of 3-dimentional reconstruction, in which the high-intensity parts of the paw are clearer and low-intensity parts show more details.

As shown in Fig. 3, Fig. 3 (a) and Fig. 3 (c) are the reconstruction results at an exposure time, Fig. 3 (b) and Fig. 3 (d) are the reconstruction results used by our method of virtual HDR via single exposure. Fig. 3 (a) and Fig. 3 (b) are the x-z sectional views. The circle mark in Fig. 3 (b) shows the strengthening of weak signals, which imply high-intensity tissues, compared with the circle mark in Fig. 3 (a). Fig. 3 (c) and Fig. 3 (d) are the x-y sectional views. The circle mark in Fig. 3 (d) shows more details compared with the circle mark in Fig. 3 (c). The outcome effect has improved image quality and enhanced the visibility of fine details, similar as HDR imaging.

And as we all known, image enhancement or improving the visual quality of image can be subjective, that is to say, one method provides a better quality image could vary from person to person. In order tomeasure the image quality after processing, the peak signal-to-noise ratio (PSNR) is used to quantitatively measure the effects of image enhancement methods on image quality. And the *PSNR* is calculated by the following functions:

$$PSNR = 20 \log_{10}\left(\frac{MAX_I}{\sqrt{MSE}}\right), \tag{6}$$

where the *MSE* (Mean Squared Error) is:

$$MSE = \frac{1}{mn}\sum_{i=0}^{m-1}\sum_{j=0}^{n-1}[I(i,j) - K(i,j)]^2. \tag{7}$$

And I represents the matrix data of the original image, K represents the matrix data of the degraded image in question, m and n respectively represents the numbers of pixels in rows and in columns, whose index is respectively represented by i and j, and MAX_I is the maximum signal value that exists in the original image. In the case of the Fig. 3's result, the recombined image is the degraded image and the value of *PSNR* is 31.12 dB, which means less distortion. A higher *PSNR* generally indicates the higher quality of the processing result, but in some cases it may not. So we can adjust the threshold value of three virtual channels based on the value of *PSNR* and visual effect to get a relatively good image quality. Then implement recombination and three dimensional reconstruction methods as described in the methods 2.2.

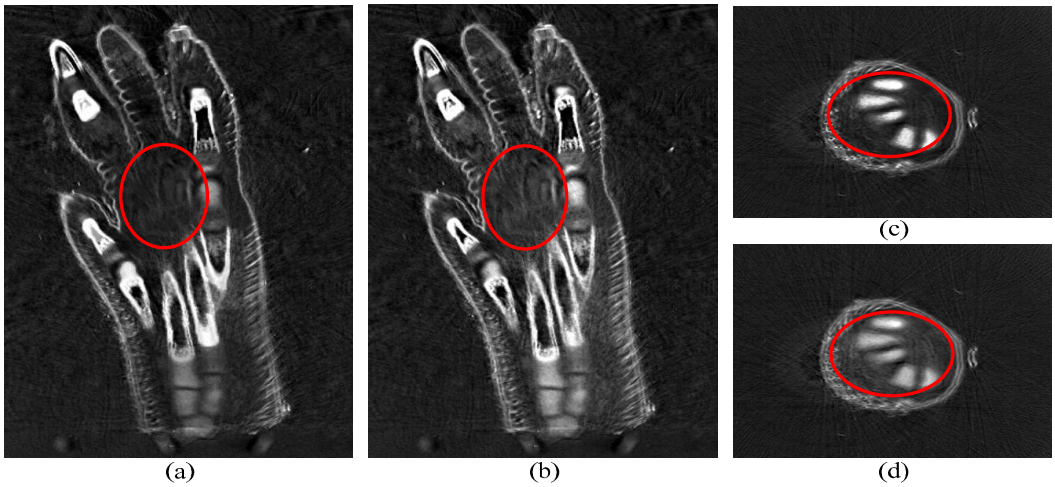

Figure 3. Results of 3-dimentional reconstruction of the mouse paw.

Strictly speaking, the proposed method is not a pure HDR imaging because three virtual channel images are created using the same original data sets, however, the outcome effect is similar in the sense that dynamic ranges are expanded. And the reconstruction result shows that the high-intensity parts are clearer and low-intensity parts show more details.

4. CONCLUSIONS

In this paper, an approach is proposed to make a trade-off between capturing weak signals and revealing more details for OPT imaging. The specimen is scanned in a single exposure and each projection image is divided into three virtual channels. The channels are recombined analogous to HDR imaging before reconstruction. The experimental results demonstrated that the proposed method improved the OPT image quality. And our future work will focus on imaging fluorescence markers of specimens by our method to expand applications.

ACKNOWLEDGMENTS

This research is supported by the National Basic Research Program of China (973 Program) under Grant 2011CB707700, the Instrument Developing Project of the Chinese Academy of Sciences under Grant No. YZ201164, the National Natural Science Foundation of China under Grant No. 81227901, 61231004, 81301346, 81027002, 81071205, 81071129, 81101095, National Key Technology R&D Program under Grant 2012BAI23B01, 2012BAI23B06, the Beijing Natural Science Foundation No. 4111004, the

Fellowship for Young International Scientists of the Chinese Academy of Sciences under Grant No. 2010Y2GA03, the Chinese Academy of Sciences Visiting Professorship for Senior International Scientists under Grant No. 2012T1G0036, 2010T2G36, 2012T1G0039, the NSFC-NIH Biomedical collaborative research program under 81261120414.

REFERENCES

[1] Sharpe, J., Ahlgren, U., Perry, P., Hill, B., Ross, A., Hecksher-Sorensen, J., Baldock, R., and Davidson, D., "Optical projection tomography as a tool for 3D microscopy and gene expression studies," Science 296(5567), 541-545 (2002).

[2] Oldham, M., Sakhalkar, H., Oliver, T., Wang, Y. M., Kirpatrick, J., Cao, Y., Badea, C., Johnson G.A., and Dewhirst, M., "Three-dimensional imaging of xenograft tumors using optical computed and emission tomography," Medical physics 33(9), 3193-3202 (2006).

[3] Kulandavelu, S., Qu, D., Sunn, N., Mu, J., Rennie, M. Y., Whiteley, K. J., Walls, J.R., Bock, N.A., Sun, J.C., Covelli, A., Sled, J.G., and Adamson, S.L., "Embryonic and neonatal phenotyping of genetically engineered mice," Ilar Journal 47(2), 103-117 (2006).

[4] Arranz, A., Dong, D., Zhu, S.P., Rudin, M., Tsatsanis, C., Tian, J. and Ripoll, J., "Helical optical projection tomography," Optics Express 21(22), 25912-25925 (2013).

[5] Fei, P., Yu, Z., Wang, X., Lu, P.J., Fu, Y., He, Z., Xiong, J. and Huang, Y., "High dynamic range optical projection tomography (HDR-OPT)," Optics Express 20(8), 8824-8836 (2012).

[6] Cheddad, A., Nord, C., Hornblad, A., Hyyrylainen, R., Eriksson, M., Georgsson, F., Vainio, S.J. and Ahlgren, U., "Improving signal detection in emission optical projection tomography via single source multi-exposure image fusion," Optics Express 21(14), 16584-16604 (2013).

[7] Arranz, A., Dong, D., Zhu, S.P., Savakis, C., Tian, J. and Ripoll, J., "In-vivo Optical Tomography of Small Scattering Specimens: time-lapse 3D imaging of the head eversion process in Drosophila melanogaster," Scientific Reports, in press, doi:10.1038/srep07325 (2014).

[8] Reinhard, E., Ward, G., Pattanaik, S. and Debevec, P., "High dynamic range imaging: acquisition, display and image-based lighting," Morgan Kaufman Publishers, San Francisco, CA, USA (2005).

[9] Gallo, O., Gelfand, N., Chen, W., Tico, M., and Pulli, K., "Artifact-free high dynamic range imaging,", 2009 IEEE International Conference on Computational Photography, San Francisco, CA, USA (2009).

[10] Ishikawa, H., Chen, C.L., Wollstein, G., Grimm, J.L., Ling, Y., Bilonick, R., Sigal, I., Kagemann, L., and Schuman, J.S., "High dynamic range imaging concept-based signal enhancement method reduced the optical coherence tomography measurement variability," Investigative Ophthalmology and Visual Science, 54(1), 836-841 (2013).

[11] Dong, D., Zhu, S.P., Qin, C.H., Kumar, V., Stein, J.V., Oehler, S., Savakis, C., Tian, J., and Ripoll, J., "Automated Recovery of the Center of Rotation in Optical Projection Tomography in the Presence of Scattering," IEEE Journal of Biomedical and Health Informatics 17(1), 198-204 (2013).

[12] Tian, J., Xue, J., Dai, Y.K., Chen, J., and Zheng, J., "A novel software platform for medical image processing and analyzing," IEEE Transactions on Information Technology in Biomedicine 12(6), 800-812(2008).

[13] Dong, D., Arranz, A., Zhu, S.P., Yang, Y.J., Shi, L.L., Wang, J., Shen, C., Tian, J. and Ripoll, J., "Vertically Scanned Laser Sheet Microscopy," Journal of Biomedical Optics 19(10), 106001(2014).